Drosophila models of pathogenic copy-number variant genes show global and non-neuronal defects during development

Yusuff *et al.*

Supplementary information

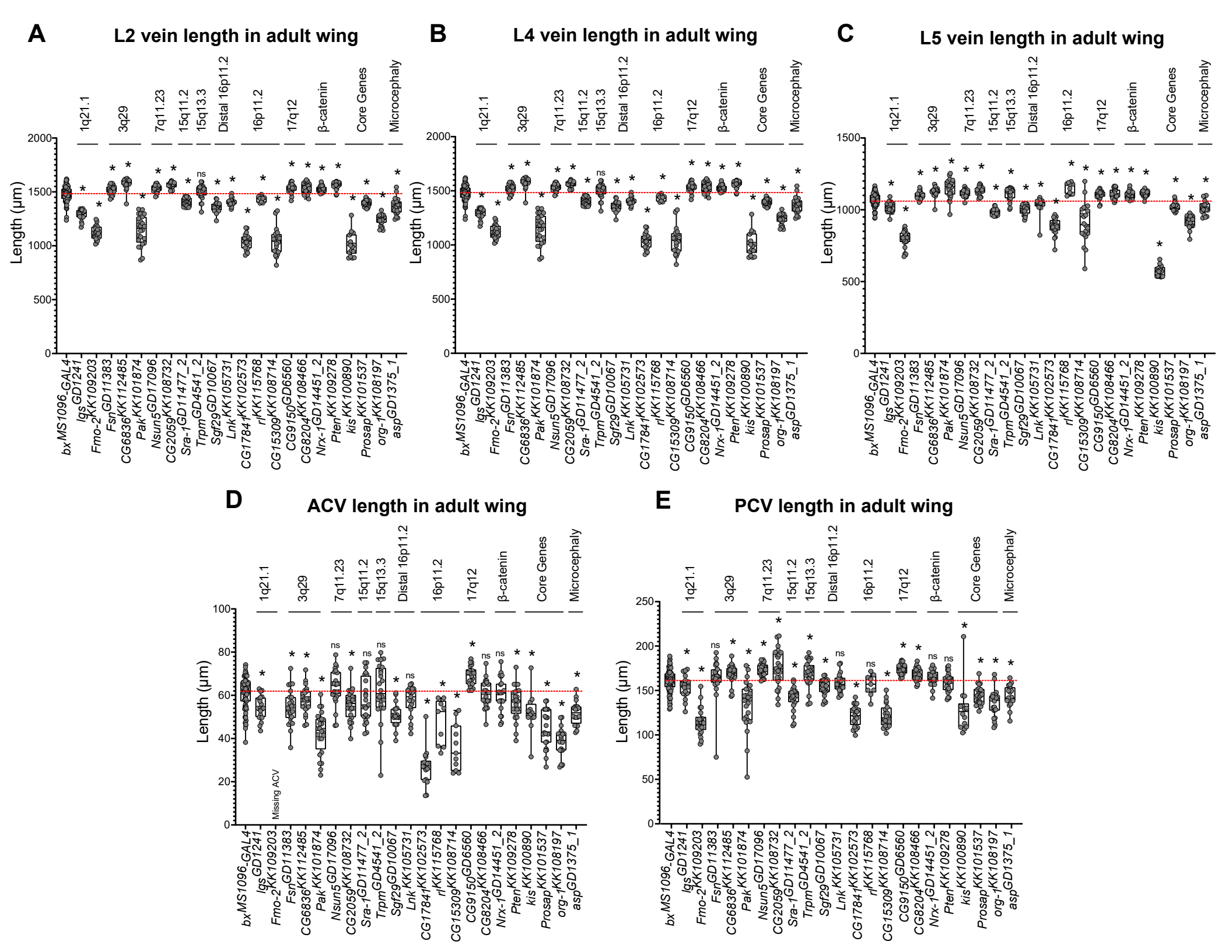
A
L2 vein length in adult wing
B
L4 vein length in adult wing
C
L5 vein length in adult wing
D
ACV length in adult wing
Missing ACV
E
PCV length in adult wing
Length (µm)
1q21.1
3q29
7q11.23
15q11.2
15q13.3
Distal 16p11.2
16p11.2
17q12
β-catenin
Core Genes
Microcephaly
bxMS1096_GAL4
lgsGD1241
Fmo-2KK109203
FsnGD11383
CG6836KK112485
PakKK101874
Nsun5GD17096
CG2059KK108732
Sra-1GD11477_2
TrpmGD4541_2
Sgf29GD10067
LnkKK105731
CG17841KK102573
rlKK115768
CG15309KK108714
CG9150GD6560
CG8204KK108466
Nrx-1GD14451_2
PtenKK109278
kisKK100890
ProsapKK101537
org-1KK108197
aspGD1375_1

Supplementary Figure 1. Quantitative vein length phenotypes for select *Drosophila* homologs of CNV and neurodevelopmental genes. Boxplots of longitudinal veins **(A)** L2, **(B)** L4, **(C)** L5, and **(D)** anterior crossvein (ACV) and **(E)** posterior crossvein (PCV) lengths for knockdown of select homologs in adult fly wings (n = 9-91, *$p < 0.05$, two-tailed Mann–Whitney test with Benjamini-Hochberg correction). All boxplots indicate median (center line), 25th and 75th percentiles (bounds of box), and minimum and maximum (whiskers), with red dotted lines representing the control median.

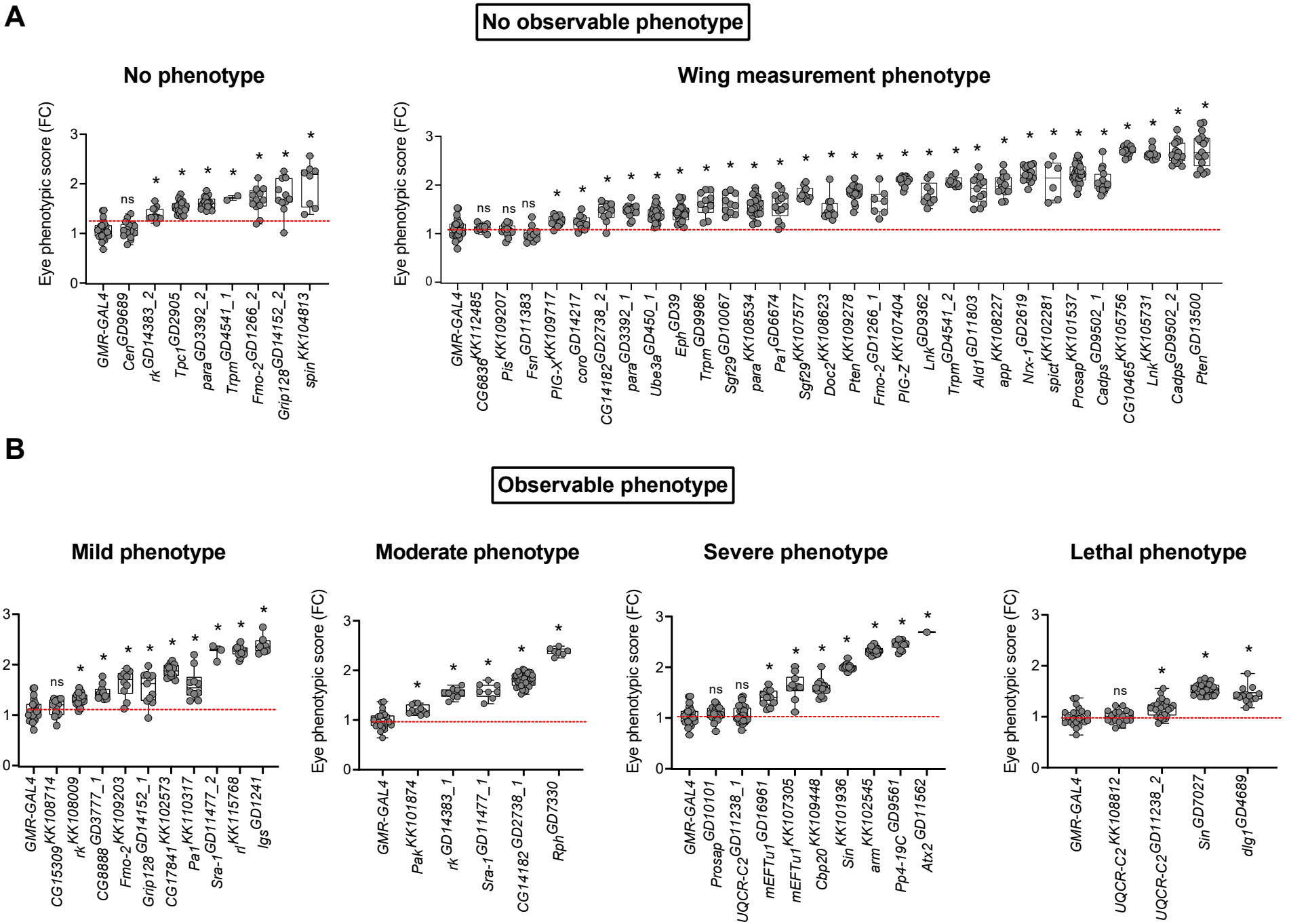
A
No observable phenotype
No phenotype
Wing measurement phenotype
Eye phenotypic score (FC)
GMR-GAL4
Cen^GD9689
rk^GD14383_2
Tpc1^GD2905
para^GD3392_2
Trpm^GD4541_1
Fmo-2^GD1266_2
Grip128^GD14152_2
spin^KK104813
CG6836^KK112485
Pis^KK109207
Fsn^GD11383
PIG-X^KK109717
coro^GD14217
CG14182^GD2738_2
para^GD3392_1
Ube3a^GD450_1
Eph^GD39
Trpm^GD9986
Sgf29^GD10067
para^KK108534
Pa1^GD6674
Sgf29^KK107577
Doc2^KK108623
Pten^KK109278
Fmo-2^GD1266_1
PIG-Z^KK107404
Lnk^GD9362
Trpm^GD4541_2
Ald1^GD11803
app^KK108227
Nrx-1^GD2619
spict^KK102281
Prosap^KK101537
Cadps^GD9502_1
CG10465^KK105756
Lnk^KK105731
Cadps^GD9502_2
Pten^GD13500
B
Observable phenotype
Mild phenotype
Moderate phenotype
Severe phenotype
Lethal phenotype
CG15309^KK108714
rk^KK108009
CG8888^GD3777_1
Fmo-2^KK109203
Grip128^GD14152_1
CG17841^KK102573
Pa1^KK110317
Sra-1^GD11477_2
rl^KK115768
lgs^GD1241
Pak^KK101874
rk^GD14383_1
Sra-1^GD11477_1
CG14182^GD2738_1
Rph^GD7330
Prosap^GD10101
UQCR-C2^GD11238_1
mEFTu1^GD16961
mEFTu1^KK107305
Cbp20^KK109448
Sin^KK101936
arm^KK102545
Pp4-19C^GD9561
Atx2^GD11562
UQCR-C2^KK108812
UQCR-C2^GD11238_2
Sin^GD7027
dlg1^GD4689

Supplementary Figure 2. Comparisons of eye-specific and wing-specific knockdowns for select *Drosophila* homologs of CNV and neurodevelopmental genes. Boxplots of *Flynotyper*-derived phenotypic scores for 66 tested adult eyes with eye-specific knockdown (*GMR-GAL4*) of select homologs of CNV and neurodevelopmental genes, normalized as fold-change (FC) to control values ($n = 1–40$, $*p < 0.05$, one-tailed Mann–Whitney test with Benjamini-Hochberg correction). RNAi lines that do not show any observable qualitative adult wing phenotypes, including lines that show wing measurement phenotypes, are represented in **(A)**, and RNAi lines with observable mild to lethal qualitative wing phenotypes are represented in **(B)**. All boxplots indicate median (center line), 25th and 75th percentiles (bounds of box), and minimum and maximum (whiskers), with red dotted lines representing the control median.

A Larval *Drosophila* expression

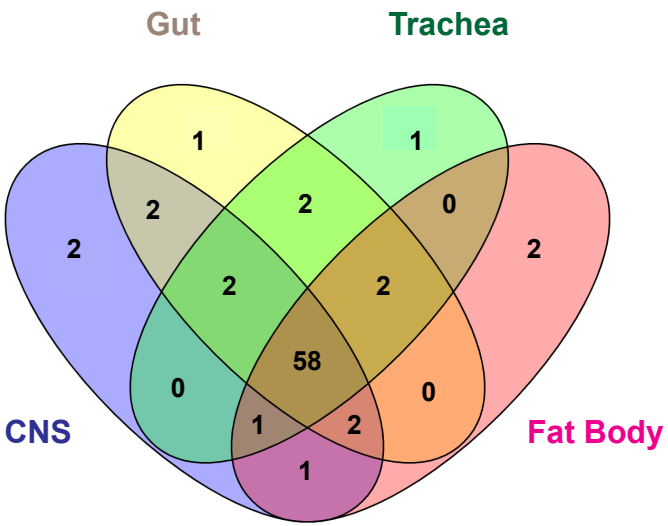

B Adult *Drosophila* expression

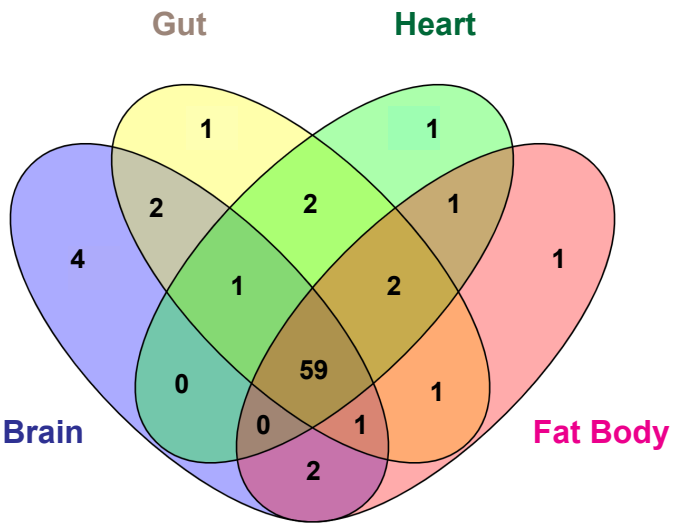

Supplementary Figure 3. Expression of *Drosophila* homologs of CNV and neurodevelopmental genes in larval and adult tissues. Venn diagrams representing the number of 76/77 tested fly homologs for CNV and neurodevelopmental genes expressed (>10 fragments per kilobase of transcript per million reads, or FPKM) in **(A)** larval (central nervous system or CNS, gut, trachea, and fat body) and **(B)** adult tissues (brain, gut, heart and fat body), are shown.

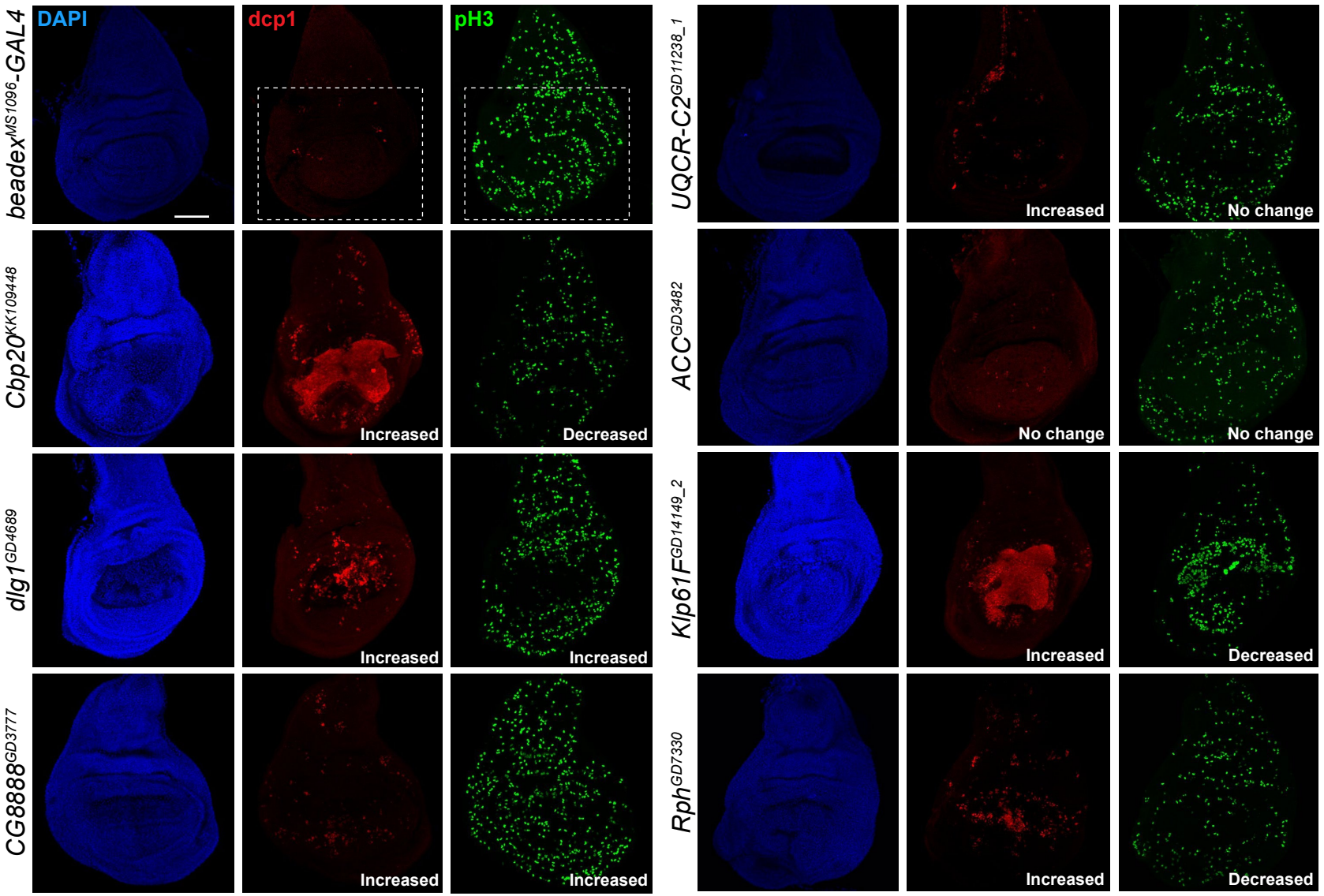
Cellular processes in larval wing discs
DAPI
dcp1
pH3
beadex^MS1096-GAL4
Cbp20^KK109448
Increased
Decreased
dlg1^GD4689
Increased
Increased
CG8888^GD3777
Increased
Increased
UQCR-C2^GD11238_1
Increased
No change
ACC^GD3482
No change
No change
Klp61F^GD14149_2
Increased
Decreased
Rph^GD7330
Increased
Decreased

Supplementary Figure 4. Additional *Drosophila* homologs of CNV and neurodevelopmental genes show altered levels of cell proliferation and apoptosis. Larval imaginal wing discs (scale bar = 50 μm) stained with nuclear marker DAPI, apoptosis marker dcp1, and cell proliferation marker pH3 illustrate altered levels of cell proliferation and apoptosis due to wing-specific knockdown of select fly homologs of CNV genes. We examined changes in the number of stained cells within the wing pouch of the wing disc (white box), which becomes the adult wing. Genotypes for the wing images are: w^{1118}/bx^{MS1096}-*GAL4;+; UAS-Dicer2/+*, w^{1118}/bx^{MS1096}-*GAL4;UAS-Cbp20*^{KK109448}*/+; UAS-Dicer2/+*, w^{1118}/bx^{MS1096}-*GAL4;+; UAS-dlg1*^{GD4689} *RNAi/UAS-Dicer2*, w^{1118}/bx^{MS1096}-*GAL4;UAS-CG8888*^{GD3777}*/+; UAS-Dicer2/+*, w^{1118}/bx^{MS1096}-*GAL4;+; UAS-UQCR-C2*^{GD11238} *RNAi/UAS-Dicer2*, w^{1118}/bx^{MS1096}-*GAL4;+; UAS-ACC*^{GD3482} *RNAi/UAS-Dicer2*, w^{1118}/bx^{MS1096}-*GAL4;UAS-Klp61F*^{GD14149}*/+; UAS-Dicer2/+*, and w^{1118}/bx^{MS1096}-*GAL4;UAS-Rph*^{GD7330} *RNAi/+;UAS-Dicer2/+*.

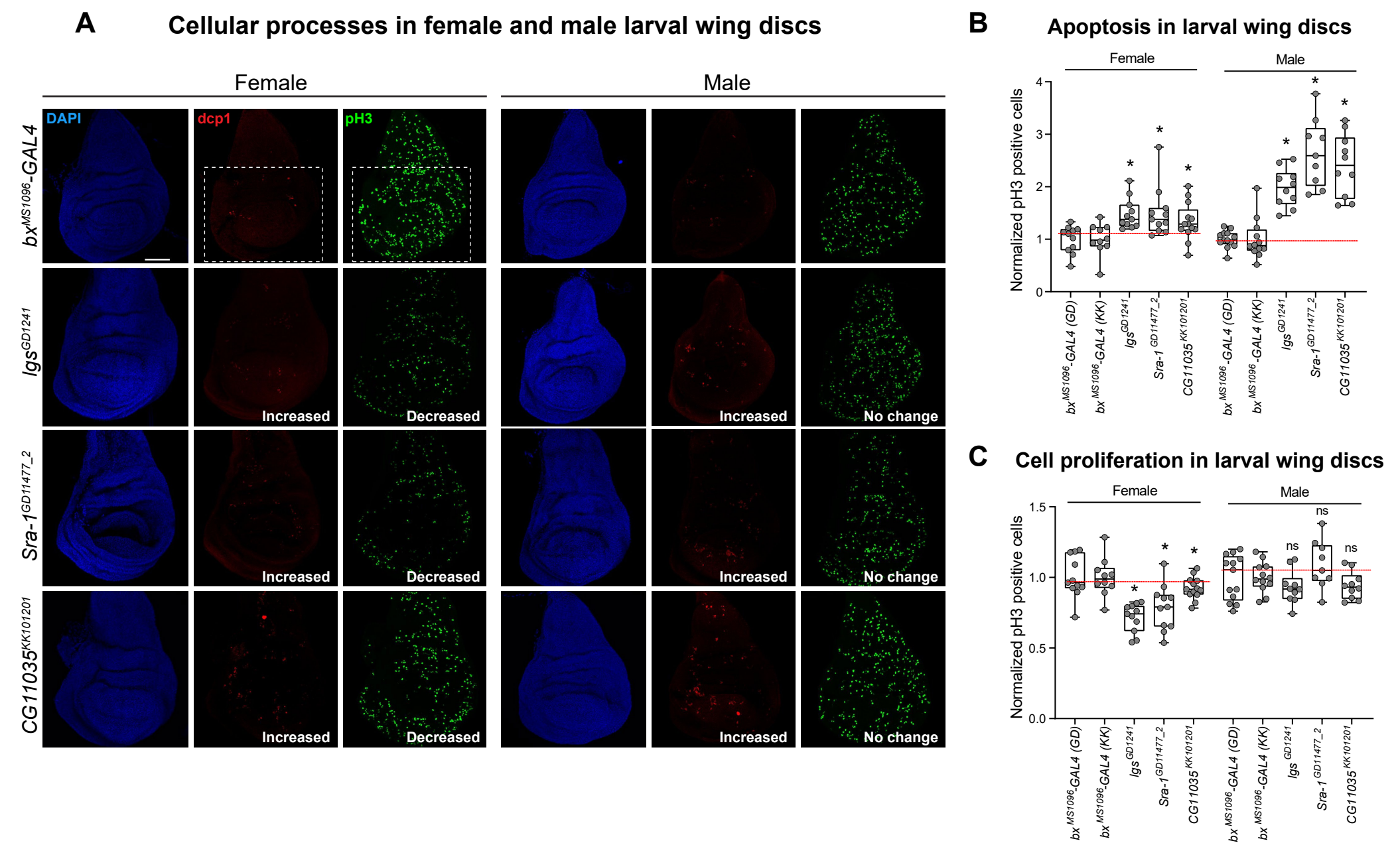
A
Cellular processes in female and male larval wing discs
Female
Male
DAPI
dcp1
pH3
bx^MS1096-GAL4
lgs^GD1241
Sra-1^GD11477_2
CG11035^KK101201
Increased
Decreased
No change
B
Apoptosis in larval wing discs
Female
Male
Normalized pH3 positive cells
0
1
2
3
4
bx^MS1096-GAL4 (GD)
bx^MS1096-GAL4 (KK)
lgs^GD1241
Sra-1^GD11477_2
CG11035^KK101201
C
Cell proliferation in larval wing discs
Female
Male
Normalized pH3 positive cells
0.0
0.5
1.0
1.5
ns

Supplementary Figure 5. Select female and male *Drosophila* homologs of CNV and neurodevelopmental genes show altered levels of cell proliferation and apoptosis. (A) Larval imaginal wing discs (scale bar = 50 μm) stained with nuclear marker DAPI, apoptosis marker dcp1, and cell proliferation marker pH3 illustrate altered levels of cell proliferation and apoptosis due to wing-specific knockdown of select fly homologs of CNV genes in females and males. We examined changes in the number of stained cells within the wing pouch of the wing disc (white box), which becomes the adult wing. Genotypes for the wing images are: w^{1118}/bx^{MS1096}-*GAL4;+; UAS-Dicer2/+*, w^{1118}/bx^{MS1096}-*GAL4;+; UAS-lgs*^{GD1241}*/UAS-Dicer2*, w^{1118}/bx^{MS1096}-*GAL4;+; UAS-Sra-1*^{GD11477}*/UAS-Dicer2*, and w^{1118}/bx^{MS1096}-*GAL4;UAS-CG11035*^{KK101201} *RNAi+; UAS-Dicer2/+*. **(B)** Box plot of dcp1-positive cells in larval wing discs with knockdown of select fly homologs of CNV and neurodevelopmental genes, normalized to controls ($n = 9–13$, $*p < 0.05$, two-tailed Mann–Whitney test with Benjamini-Hochberg correction). The number of dcp1 positive cells were calculated manually. **(C)** Box plot of pH3-positive cells in the larval wing discs with knockdown of select fly homologs of CNV and neurodevelopmental genes, normalized to controls ($n = 9–13$, $*p < 0.05$, two-tailed Mann–Whitney test with Benjamini-Hochberg correction). The number of pH3 positive cells were calculated using the AnalyzeParticles function in ImageJ. All boxplots indicate median (center line), 25th and 75th percentiles (bounds of box), and minimum and maximum (whiskers), with red dotted lines representing the control median.

Disruption of signaling pathways in larval wing discs

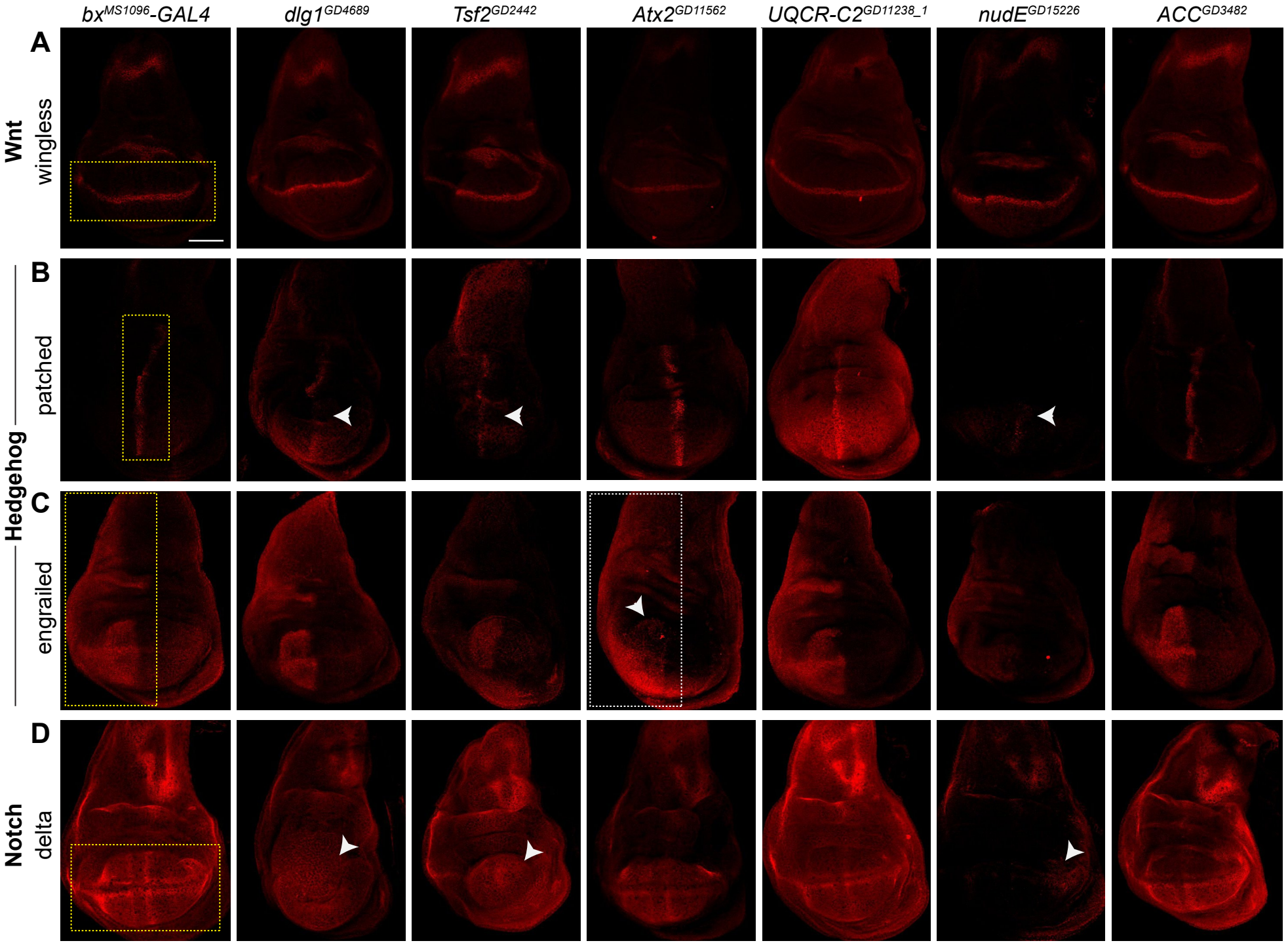

Supplementary Figure 6. Additional *Drosophila* homologs of genes within CNV regions interact with conserved signaling pathways to induce developmental phenotypes. Larval imaginal wing discs (scale bar = 50 μm) stained with **(A)** wingless, **(B)** patched, **(C)** engrailed, and **(D)** delta illustrate disrupted expression patterns for proteins located within the Wnt (wingless), Hedgehog (patched and engrailed), and Notch (delta) signaling pathways due to wing-specific knockdown of additional fly homologs of CNV and neurodevelopmental genes. Dotted yellow boxes represent expected expression patterns for signaling proteins in bx^{MS1096}*-GAL4* control images. White arrowheads and dotted white boxes highlight disruptions in expression patterns of signaling proteins with knockdown of CNV or neurodevelopmental genes. Genotypes for the wing images are: w^{1118}/bx^{MS1096}*-GAL4;+; UAS-Dicer2/+*, w^{1118}/bx^{MS1096}*-GAL4;+; UAS-dlg1*^{GD4689} *RNAi/UAS-Dicer2*, w^{1118}/bx^{MS1096}*-GAL4;+; UAS-Tsf2*^{GD2442} *RNAi/UAS-Dicer2*, w^{1118}/bx^{MS1096}*-GAL4;+; UAS-Atx2*^{GD11562} *RNAi/UAS-Dicer2*, w^{1118}/bx^{MS1096}*-GAL4;+; UAS-UQCR-C2*^{GD11238} *RNAi/UAS-Dicer2*, w^{1118}/bx^{MS1096}*-GAL4;+; UAS-nudE*^{GD15226} *RNAi/UAS-Dicer2*, and w^{1118}/bx^{MS1096}*-GAL4;+; UAS-ACC*^{GD3482} *RNAi/UAS-Dicer2*.


A
Human CNV genes interact with Wnt signaling pathway genes in multiple tissues
Kidney
Heart
Brain
PPP4C
KIF11
AATF
NCBP2
POLR3E
B
Human CNV genes interact with Hedgehog signaling pathway genes in multiple tissues
Kidney
Heart
Brain
NDE1
DLG1
ATXN2L
MFI2
CNV/neurodevelopmental gene
Signaling pathway gene
Connector gene

Supplementary Figure 7. Tissue-specific network diagrams showing connectivity of human CNV genes with conserved signaling pathway genes. Representative network diagrams of nine human CNV and neurodevelopmental genes whose fly homologs disrupt the **(A)** Wnt and **(B)** Hedgehog signaling pathway and 162 human Wnt and 46 human Hedgehog signaling genes within kidney, heart, and brain-specific gene interaction networks are shown. Yellow nodes represent CNV and neurodevelopmental genes, pink nodes represent Notch signaling pathway genes, and green nodes represent connector genes within the shortest paths between CNV and Notch pathway genes.

Supplementary Data 1 (Excel file). *Drosophila* homologs of human CNV and neurodevelopmental genes as determined using DIOPT v.7.1.

Supplementary Data 2 (Excel file). Qualitative and quantitative adult wing phenotypic data for *Drosophila* homologs of human CNV and neurodevelopmental genes. This file shows the raw frequencies of severity for the five qualitative wing phenotypes and average areas and vein lengths for all 136 female and male tested RNAi lines. In addition, this file also includes k-means clustering analysis for the female RNAi lines.

Supplementary Data 3 (Excel file). Summary of adult wing qualitative and quantitative phenotypes by *Drosophila* homologs. This file summarizes qualitative k-means clustering and longitudinal L3 vein length and wing area changes for all 136 RNAi lines by fly homologs. We define discordant homologs when RNAi lines for the same homologs showed inconsistent wing phenotypes. For each homolog with multiple RNAi lines, we checked discordance among RNAi lines for no phenotype versus any qualitative or quantitative phenotypes, followed by discordance for small or large quantitative phenotypes.

Supplementary Data 4 (Excel file). Phenotypes of mouse knockdown models for homologs of CNV genes. This file lists lethality and neuronal and non-neuronal phenotypes, categorized using top-level Mammalian Phenotype Ontology terms, for knockdown models of 130 mouse homologs of CNV genes derived from the Mouse Genome Informatics (MGI) database.

Supplementary Data 5 (Excel file). Summary of eye-specific and wing-specific phenotypes for fly homologs. This file summarizes eye-specific and wing-specific phenotypes by severity category for 66 RNAi lines by fly homologs of CNV and neurodevelopmental genes. Eye phenotype severity is defined by *Flynotyper* phenotypic scores with fold-change (FC)

normalization to control as follows: no change (0–1.1 FC), mild (1.1–1.5 FC), moderate (1.5–2.0 FC), and severe (>2.0 FC). Wing phenotype severity is defined by k-means clustering for qualitative phenotypes and quantitative size changes as listed in **Supp. Data 3**.

Supplementary Data 6 (Excel file). Tissue-specific expression of *Drosophila* homologs and human CNV and neurodevelopmental genes. This file lists expression values across multiple fly and human tissues for all 79 *Drosophila* homologs and 150 human genes. Fly expression data (fragments per kilobase of transcript per million reads, or FPKM) was derived from the FlyAtlas Anatomical Microarray dataset, and human expression data (transcripts per million reads, or TPM) was derived from the Genotype-Tissue Expression (GTEx) dataset v.1.2.

Supplementary Data 7 (Excel file). Summary of immunostaining of the larval imaginal wing discs. This file summarizes changes in apoptosis (27 homologs), cell proliferation (27 homologs), and Wnt, Hedgehog, and Notch signaling pathway proteins (14 homologs), along with qualitative and quantitative adult wing phenotypes (as listed in **Supp. Data 2.**), for female and male fly homologs.

Supplementary Data 8 (Excel file). Tissue-specific network connectivity for candidate CNV genes and signaling pathway genes. This file lists the shortest path lengths between nine candidate CNV genes and 265 genes within Wnt, Hedgehog, and Notch signaling pathways for heart, kidney, and brain-specific gene interaction networks, along with the connector genes that are within the shortest paths. Enriched Gene Ontology (GO) Biological Process, Cellular Component, and Molecular Function terms for sets of connector genes for each signaling pathway in each tissue-specific networks are also represented.

Supplementary Data 9 (Excel file). List of *Drosophila* stocks used for experiments, including stock numbers and genotypes.

Supplementary Data 10 (Excel file). Statistics for all experimental data. This file shows all statistical information (sample size, mean/median/standard deviation of datasets, test statistics, p-values, degrees of freedom, confidence intervals, and Benjamini-Hochberg FDR corrections) for all data. Statistical information for Kruskal-Wallis test includes factors, degrees of freedom, test statistics, and post-hoc pairwise Wilcoxon tests with Benjamini-Hochberg correction.